Mechanically Stable Solution-Processed Transparent Conductive Electrodes for Optoelectronic Applications

Milad Kianpisheh[a], , *Bahareh Rezaei*[b], *Zahra Babaei*[a], *Kamal Asadi*[c,d], *Faramarz Afshar-Taromi*[a*], *Hamed Sharifi Dehsari*[c*]

[a] Department of Polymer Engineering and Color Technology, Amirkabir University of Technology, P.O.Box-15875-4413, Tehran, Iran. E-mail: afshar@aut.ac.ir; Tel: +982164542401.

[b] Department of Chemistry, Amirkabir University of Technology, Tehran, Iran.

[c] Max Planck Institute for Polymer Research Ackermannweg 10, 55128 Mainz, Germany. E-mail: h.sharifi1989@gmail.com

[d] Department of Physics, University of Bath, Claverton Down, Bath, BA2 7AY, United Kingdom

KEYWORDS: Ag Nanowires, PEDOT:PSS, Flexible Electrodes, Polymer Solar Cell, Polymer-Surfactant, mechanical stability

ABSTRACT

The bilayer structure of poly(3,4-ethylenedioxythiophene):poly(styrene sulfonate) (PEDOT:PSS) coating on silver nanowires (AgNWs) film is a promising structure for replacing indium tin oxide (ITO) as a flexible transparent conductive electrode. Pristine PEDOT:PSS film due to its hydrophilicity and high permeability cannot fully protect AgNWs from mechanical stress and oxidation. Here, we present a composite approach that improves mechanical properties and lifespan of the AgNWs/PEDOT:PSS electrode by adding polyvinyl alcohol (PVA) as a polymer-surfactant. It is shown that addition of PVA improves the conductivity as well as the stability of

hybrid electrode under demanding mechanical stress conditions. The drop in conductivity of the hybrid electrode is only 17% after 2000 repeated bending cycles whereas the reference electrode has shown a dramatic drop of 180% in the conductivity. We speculate that generation of hydrogen bonds between PEDOT:PSS and PVA increases adhesivity and cohesivity of the conductive polymer film to the sublayer. So PEDOT:PSS-PVA film not only fixes the arrangement of AgNWs but also improves the welding on cross junction points. By addition of PVA, optoelectronic performance (Figure-of-merit (Φ_{TC})) of the electrode is improved from $\Phi_{TC} = 2.646\times10^{-3}\ \Omega^{-1}$ for AgNWs/PEDOT:PSS to $\Phi_{TC} = 3.819\times10^{-3}\ \Omega^{-1}$ for AgNWs/PEDOT:PSS-PVA electrode and power conversion efficiency (PCE) of the polymer solar cell (PSC) is increased by over 17%.

1. INTRODUCTION

Transparent conductive electrode (TCE) is an essential constituents in the construct of all optoelectronic devices such as solar cells, light-emitting diodes (LEDs), and smart windows [1–4]. For application in flexible electronics, electrodes that made of metal oxides pose severe constraints because of their high brittleness upon bending, the difficulty of processability on plastic substrates, and their high price [1,5]. Three categories of materials including metal nanostructures such as nanowires [6], carbon derivatives such as multi-walled carbon nanotubes (MWCNTs) [7] and graphene [8], as well as conductive polymers such as PEDOT:PSS [9] are recommended to replace metal oxides [5,10]. But each of the alternative materials has limitations and shortcomings.

A thin layer of metal nanowires, in particular silver nanowires (AgNWs) is a promising candidate due to its high conductivity, excellent bending performance[11], and low adverse effect on the transmittance of the electrode[12]. Despite the unique advantages of AgNWs, it has some disadvantages like high wire-to-wire junction resistance, high environmental instability, high surface roughness, poor adhesion to substrates [6,11,13] and weak charge transfer across the empty space between adjacent AgNWs [12]. The significant difference in mechanical properties between the nanowires and polymeric flexible substrates, causes delamination of silver nanowire electrodes upon cyclic stretching or bending [14]. Several strategies such as thermal treatments [15], humidity assisted annealing [16], mechanical pressing [17] and plasmonic welding [18] have been proposed to overcome the limitations. Alternatively, a hybrid structure is proposed, where AgNWs is integrated with a conductive polymers or carbon nanostructures such as graphene in a double-layer or sandwich structures [1,12,19–21]. The presence of coating layer on top of the AgNWs, reduces

the roughness [11,22], fills the voids between the nanowires, and increases the conductivity of the electrode by creating welding on cross junctions of AgNWs [12]. It also reduces the oxidation rate of silver nanowires and increases the stability [23].

PEDOT:PSS, is a common conductive polymer that's used as a coating layer of AgNWs electrode due to its good processability, suitable cost, excellent thermal stability and good optical properties [9]. Despite all the unique benefits, PEDOT:PSS shows low conductivity before doping process [9], hygroscopic properties [24], instability of properties in long periods [25] and brittleness of the films [14,26–28]. It has been shown that, the conductivity of PEDOT:PSS can be improved through addition of polar solvents [29,30], anionic [31] and non-ionic surfactant [32] and graphene based derivatives [25,33]. Unfortunately, most of the above mentioned methods have little effect on improving mechanical properties and reducing permeability, even in some cases, it adversely affects the flexibility of the PEDOT:PSS films [11,28]. One way to improve the mechanical properties of PEDOT:PSS is to swell it resulting in a relatively large gap between PEDOT coils and PSS coils [34]. Plasticizers and soft materials are recommended to bridge the gap between the two polymer parts [34]. For example, addition of Zonyl fluorosurfactant (Zonyl) and Triton X100, not only increase the electrical conductivity, but also partially improve the mechanical properties of PEDOT:PSS films[17,35].

In spite of all the researches done to improve the properties of PEDOT:PSS films as a conductive protective layer for metal nanowire electrodes, there is still a need for a single step and low-cost multipurpose method. A method that beside improving the conductivity level and maintaining transmittance, it also drastically enhances the mechanical properties of the film and greatly improves the stability by reducing the permeability to the air and moisture. In this work, we introduce a new method to improve PEDOT:PSS film properties as a coating layer in bilayer electrode of AgNWs/PEDOT:PSS by addition of polymer-surfactant. To increase the conductivity, DMSO as a cosolvent and PVA as a polymer-surfactant were added to the PEDOT:PSS solution. Addition of cosolvent and polymer surfactant at an optimal concentration prevent the migration of surfactant chains to the surface of the film. So, in addition to changing the properties of PEDOT:PSS film from brittle to ductile, increased the conductivity level of it. Presence of PVA in coating film improved the adhesion of it to the surface and fixed the arrangement of AgNWs in mechanical stresses. We observe that figure of merits improves from $\Phi_{TC} = 2.646\times10^{-3}\ \Omega^{-1}$ for AgNWs/PEDOT:PSS/DMSO to $\Phi_{TC} = 3.819\times10^{-3}\ \Omega^{-1}$ for AgNWs/PEDOT:PSS/DMSO/PVA

electrode. Appling the new bilayer electrode in PSCs structure increased the efficiency by 17% compared to the AgNWs/PEDOT:PSS/DMSO electrode.

2. EXPERIMENT SECTION

2.1. Materials

Silver nitrate (≥99.0%), Polyvinylpyrrolidone (PVP) (M_W= 360000 g/mol) and $FeCl_3.6H_2O$ that used in the synthesis of silver nanowires, Poly(vinyl alcohol) (M_W= 31,000-50,000 g/mol, 87-89% hydrolyzed) ,poly (3-hexylthiophene-2,5-diyl) (P_3HT) and [6,6]-phenyl C_{61}butyric acid methyl ester ($PC_{61}BM$) is provided by Sigma-Aldrich. PEDOT:PSS (Clevios™ PH 1000 for coating layers fabrication and Clevios™ PVP AI 4083 for hole transport layer fabrication) were purchased from Heraeus. All solvents were purchased from Merck. All chemicals were used without further purification.

2.2. Synthesis of silver nanowires

Silver nanowires were synthesized with polyol method [36,37]. Briefly, a solution of 0.12 mol/L of silver nitrate and a solution of 4.44×10^{-5} mol/L of PVP in ethylene glycol were prepared separately. 10 ml of each solution was mixed together. 5 ml of the $FeCl_3.6H_2O$ in ethylene glycol at a concentration of 0.12 g/L was added to the above mixture and was stirred vigorously at ambient temperature for 3 min. Then it was transferred to the balloon with two spouts at 140 °C and was restored to reflux for 3 h until the color of the suspension changed from colorless to silver.

Afterward, the purification of synthesized nanowires in ethylene glycol was done by centrifugation for 4 min with 4000 rpm. In the next step, the suspension in ethanol was centrifuged for 3 min at a speed of 3000 rpm for full purification. Finally, purified AgNWs were dispersed in ethanol. The characterization tests of synthesized AgNWs are explained in **Supporting Information (SI)**.

2.3. Fabrication of coating layers

First, PEDOT:PSS (Clevios™ PH 1000) aqueous solution was filtered through a syringe filter (0.45 μm pore size). Then 6 wt% DMSO was added to the PEDOT:PSS solution and stirred for 4 h. Different weight percentages from 0 to 0.25 wt% of PVA were added to the polymer solutions

and stirred at 70 °C for 24 h. Thin films were obtained by spin coating the solutions followed by annealing at 120 °C for 15 min.

2.4. Fabrication of bilayer electrodes

AgNWs suspension was diluted with ethanol to various concentrations (1 to 6 mg/ml in ethanol) and was shaken for a few minutes before using. These suspensions were spin coated on cleaned glasses or polyethylene terephthalates (PET) at 900 rpm for 30 s and 1500 rpm for 2 min. Fabricated films were annealed at 70 °C in nitrogen atmosphere for 10 min to remove the residual solvent. Then coating layers with 100 nm thickness were applied on AgNWs films separately. Finally, fabricated bilayer electrodes were placed at 70 °C for 10 min. The schematic description of the above process is shown in the **scheme 1**.

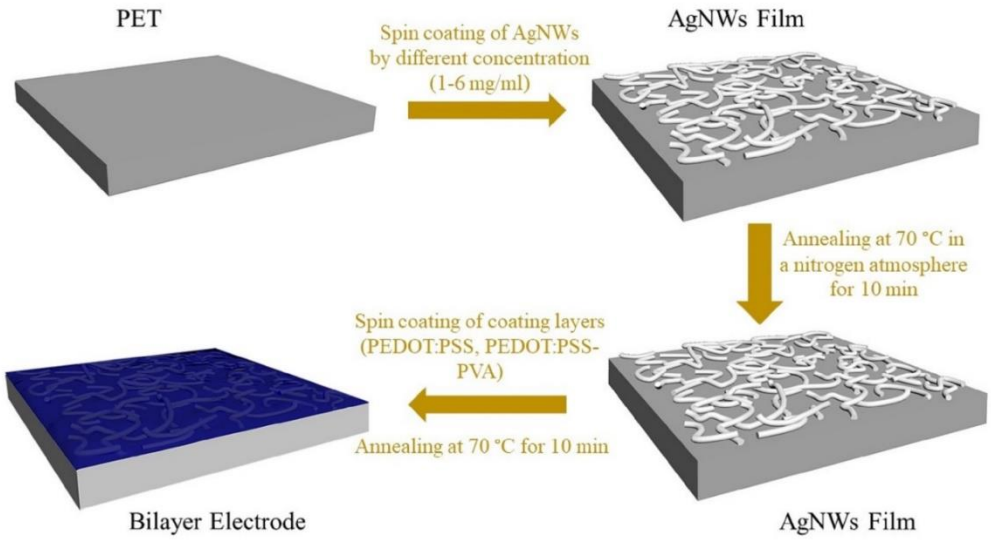

Scheme 1. Schematic description of the bilayer electrode fabricating process

2.5. Evaluation of the mechanical properties of electrodes

To evaluate the mechanical properties of electrodes, static and dynamic mechanical bending tests were performed. For dynamic mechanical bending test, rectangular samples with the dimensions of 3 cm×1 cm were used. The relative sheet resistance (R_S/R_{S0}) of electrodes on polyethylene terephthalate (PET) substrates during 2000 bending cycles with bending radius of 2 mm (angle of 180°) were measured. For static mechanical bending test, the square samples with

the dimensions of 3 cm×3 cm were used. The relative sheet resistance (R_S/R_{S0}) of electrodes on PET substrates during 90 min under 180° bending were measured.

2.6. Polymer solar cell fabrication

PSCs were fabricated using all three types of electrodes (AgNWs, AgNWs/PEDOT:PSS and AgNWs/PEDOT:PSS-PVA). All of the PSCs were fabricated with the same device structure of substrate/ TCE (200 nm) / hole transporting material (PEDOT:PSS) (90 nm) / active layer (P3HT:PCBM) (180 nm) / cathode (AL) (100 nm). PEDOT:PSS (Clevios™ PVP AI 4083) was stirred for 15 min at 40 °C and then was filtered through a syringe filter (0.45 μm pore size). 100 μl of the prepared solution was spin coated at 2000 rpm for 1 min on the electrode (AgNWs/PEDOT:PSS or AgNWs/PEDOT:PSS-PVA), and it was annealed at 70 °C for 20 min to form the hole transport layer. In the next step, the solution of P3HT (10 mg/ml) and PCBM (10 mg/ml) in dichlorobenzene were mixed and spin coated in the glove box at 1000 rpm for 1 min and subsequently annealed at 70 °C. Then, Cathode (Al) was coated by a physical vapor deposition (PVD) method with a deposition rate of 0.2 nm/s and thickness of 100 nm. Shadow mask with an active area of 0.5 cm^2 was used to design the Al pattern.

2.7. Characterization of prepared electrodes and PSCs

The sheet resistance of thin films was measured by a 4-point probe resistivity measurement system (Sanat Nama Javan Co. FPP-SN-554). Optical transmittance was evaluated using a Shimadzu uv-3600 Spectrophotometer. Raman spectra were obtained using TakRam N1-541 Raman system, using 532 nm laser wavelength. X-ray diffraction(XRD) patterns of the samples were recorded with PHILIPS PW1730 X-ray diffractometer, using Cu-Kα radiation (λ =1.54056 Å) at 40 kV and 30 mA with a step size of 0.05°. Scanning electron microscope (SEM) (SERONTECHNOLOGIES AIS2100) images for proving AgNWs synthesis, analytical study of synthesized silver nanowires, and also surface and fracture analysis of the electrodes after bending test were used. Atomic force microscopy (AFM) (ENTEGRA AFM NT-MDT) was used to study the surface morphology of conductive thin films. J–V curves were measured using a solar simulator (IRASOL Co) with an incident light intensity of 100 mW cm^{-2} (AM 1.5 G light source).

3. RESULT AND DISCUSSION

3.1. Investigation and optimization of polymer coating

To optimize the concentration of polymer-surfactant, the conductivity of fabricated thin films was measured. Addition of 6 wt% DMSO to the aqueous solution of PEDOT:PSS, increases the conductivity of the film from 0.3 S/cm to 520 S/cm. **Figure 1(a)** shows the trend of growing conductivity by addition of polymer-surfactant up to a concentration of 0.1 wt% of PVA up to more than 830 S/cm. On the other side addition of PVA slightly reduces the transmittance of the electrodes as illustrated in **Figure 1(b).** The transmittance of the PEDOT:PSS/ 6% DMSO/ 0.1% PVA and PEDOT:PSS/ 6% DMSO films are amounted to 88.7% and 91.7% at 550 nm wavelength, respectively. In this study, the range of 400 to 750 nm (visible range) was selected to investigate light transmittance. Because as shown in Figure S1, absorption spectra of silver nanowires indicate absorption peaks in the range of 300 to 400 nm. Which is caused severe irregularities at transmittance spectrum of electrodes. On the other hand, the light absorption range in polymer Photoactive materials such as P3HT:PCBM is typically limited to less than 750 nm [38,39]. In the following, the names of PEDOT:PSS/6%DMSO and PEDOT:PSS/6% DMSO/ 0.1% PVA coating layers are abbreviated to PEDOT:PSS and PEDOT:PSS-PVA.

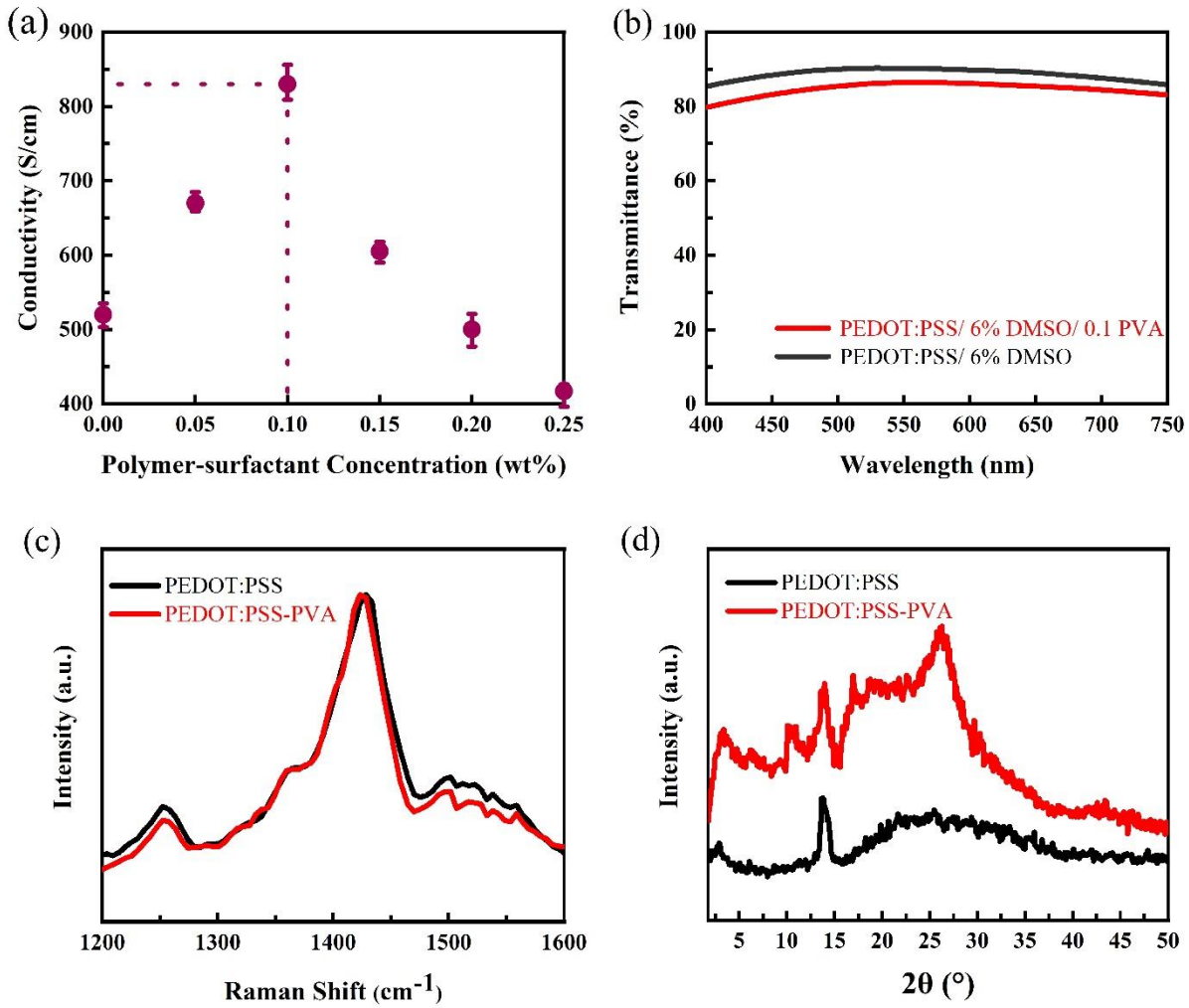

Figure 1. (a) Conductivity of thin films versus different concentrations of polymer-surfactant. **(b)** Transmission spectra of PEDOT:PSS/6 wt% DMSO and PEDOT:PSS/6 wt% DMSO/0.1 wt% PVA at 400–750 nm wavelength range. **(c)** Raman spectra of PEDOT:PSS and PEDOT:PSS- PVA coating films at 1200–1600 nm wavelength range. **(d)** XRD patterns of PEDOT:PSS and PEDOT:PSS- PVA coating films

Figure-of-merit (Φ_{TC}) as defined by Haacke [40] , is used to evaluate optoelectronic properties of coatings:

$$\Phi_{TC} = \frac{T_{550}^{10}}{R_s} (\Omega^{-1}) \quad (1)$$

$\Phi_{TC} = 2.512\times10^{-3}\ \Omega^{-1}$ for PEDOT:PSS-PVA and $\Phi_{TC} = 2.189\times10^{-3}\ \Omega^{-1}$ for PEDOT:PSS are calculated. Despite the slight drop in transmittance, an increase in Φ_{TC} is observed due to the increase in the conductivity level of the films.

The extremum amount of conductivity is attributed to the maximum amount of PEDOT:PSS coils opening and the highest separation of conductive $PEDOT^+$ from insulating PSS^-. Because the conductivity of PEDOT:PSS are strongly dependent on the film morphology. The morphology of PEDOT:PSS in the pristine form is in the coil structure. In such a way that the conductive chains ($PEDOT^+$) are surrounded by insulate coil chains (PSS^-) [9,41]. Therefore, this morphological structure greatly reduces the conductivity of the PEDOT:PSS film. By changing the conformation to linear structure, the PEDOT chains are released from the blockade of PSS. Besides, with increasing molecular orientation, the crystallinity and packing of the chains also increases. So, changing the conformation of PEDOT:PSS from coils to linear structure facilities electron transfer between PEDOT chains and significantly increases the conductivity of the PEDOT:PSS film [9,42]. However, as shown in transmission spectra (**Figure 2 (b)**) reduces the transmittance of polymer coating. AFM analysis (detailed in **SI, Figure S2**) and Raman spectra are used to demonstrate the change of PEDOT chains from coil to linear structure by addition of polymer surfactant. **Figure 1(c)** shows the Raman spectra of both coating films in the range 1200 to 1600 cm^{-1}. The main peak of PEDOT:PSS coating film represents at 1433 cm^{-1}. This peak is related to Symmetric Cα=Cβ stretching band [43,44]. By adding PVA to the PEDOT:PSS/DMSO film, a red shift from 1433 to 1428 cm^{-1} for this peak is observed in the polymer spectrum. This shift can be related to the change of conformation from benzoid (coil conformation) to quinoid structure (expanded coil or linear conformation) [43,44]. Therefore, addition of the polymer surfactant after adding DMSO by increasing the ratio of the linear to the coil conformation of PEDOT structures has been able to increase the conductivity of the polymer film more than addition of the solvent alone. At concentrations greater than 0.1 wt% of PVA, the decrease in the conductivity level is observed. This is attributed to the decrease of coulombic repulsions among the negative charges of PSS^- due to reduced concentration of PSS^- at the surface of polymer-surfactant chains and thus reduction of extension of PEDOT:PSS coils [32]. In addition, the decrease of conductivity can be related to the increase of non-conductive parts (PVA), and also imprisonment of the $PEDOT^+$ chains in the middle of the insulator section.

Figure 1(d) shows XRD patterns obtained from each coating layer. By comparing patterns, changes in the crystal structures of the coatings by the addition of PVA are demonstrated. As stated in various research, PEDOT:PSS XRD pattern has several peaks. The most important peaks for studying the crystal structures and electrical conductivity of PEDOT:PSS/DMSO films are observed in the ranges of $2\theta = 2.9°$ and 25.74° [45–47]. By using Bragg's law, these angles are related to spacings of approximately 30.44 and 3.45 Å, respectively. The long lamella stacking distance (30.44 Å) can be attributed to the alternate lamella stacking distance of PEDOT and PSS in the plane ($d_{(100)}$) [45–47]. According to previous studies, this distance in the pristine PEDOT:PSS has been reported in the range of 23 Å [41-44]. This result is compatible with the total width of PEDOT (= 7.5 Å) and PSS (= 15.5 Å) based on chemical structures of them [45,48]. Therefore, by addition of DMSO, increasing the distance between the PEDOT and PSS chains and creating an empty space between them is proved. Another d spacing (3.45 Å) Represents the distance between π-π stacking ($d_{(010)}$) of the PEDOT thiophene ring [45–47]. By reducing this distance while increasing molecular packing and local crystallinity, electron transfer between PEDOT chains becomes easier and conductivity increases [45–47]. In PEDOT:PSS-PVA film , $d_{(100)}$ and $d_{(010)}$ peaks are shifted to $2\theta = 3.12°$ (28.29 Å) and 26.24° (3.39 Å) respectively, and the intensity of them increases. Therefore, the addition of PVA, increases the amount of crystallinity and conductivity of the coating film. Another important parameter that changed by addition of PVA was related to the shifting of $d_{(100)}$ peak from 30.44 Å to 28.29 Å. As mentioned above, this peak is related to the lamella stacking distance of PEDOT and PSS in the plane and reducing it decreases the free space between PEDOT and PSS. Hydrogen bonding between PEDOT:PSS and PVA has been reported in various research in the past [49–51]. therefore, this free space reduction can be attributed to the formation of hydrogen bond between PEDOT:PSS and PVA chains.

So, Adding PVA to the polymer coating, by increasing the crystallinity, molecular packing between PEDOT chains and reducing the gap between PEDOT and PSS chains in addition to decreasing the transmittance (**Figure 1(b))** , it can also reduce the permeability of the polymer layer and improve the stability of the electrode's properties.

3.2. Design and optimization of prepared electrodes

Applied coatings top of the AgNWs films simultaneously affect optical and electrical properties of the films. **Figure 2(a)** and **(b)** shows the transmittance spectra and sheet resistance

of the electrodes with the PEDOT:PSS coating layer whereas **Figure 2(c)** and **(d)** shows the ones with the PEDOT:PSS-PVA coating layer.

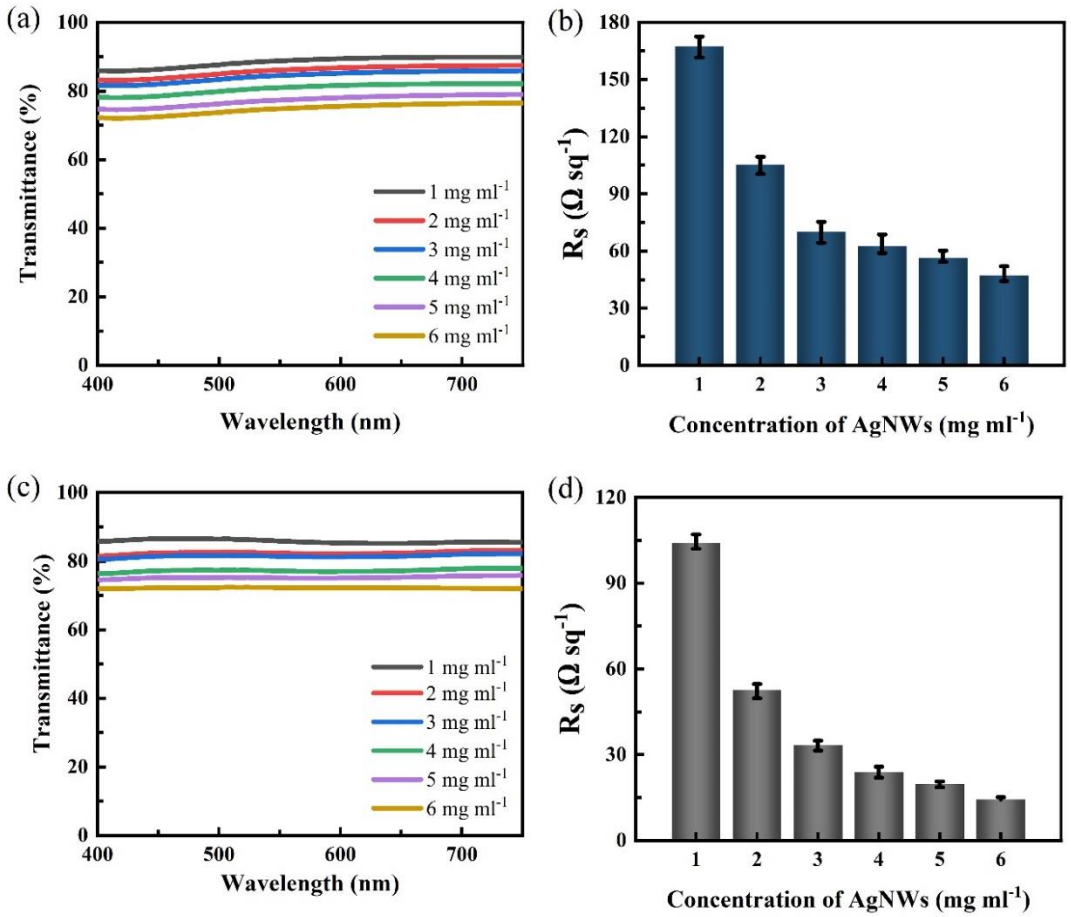

Figure 2. Transmission spectra of **(a)** AgNWs/PEDOT:PSS **(c)** AgNWs/PEDOT:PSS-PVA electrodes at the 400–750 nm wavelength range. R_s Histograms of **(b)** AgNWs/PEDOT:PSS **(d)** AgNWs/PEDOT:PSS-PVA electrodes as a function of AgNWs suspension concentration (1 mg/ml to 6 mg/ml).

The Φ_{TC} values for each electrode with PEDOT:PSS and PEDOT:PSS-PVA coating layers as a function of different concentrations of AgNWs are calculated and are shown in **Figure 3.**

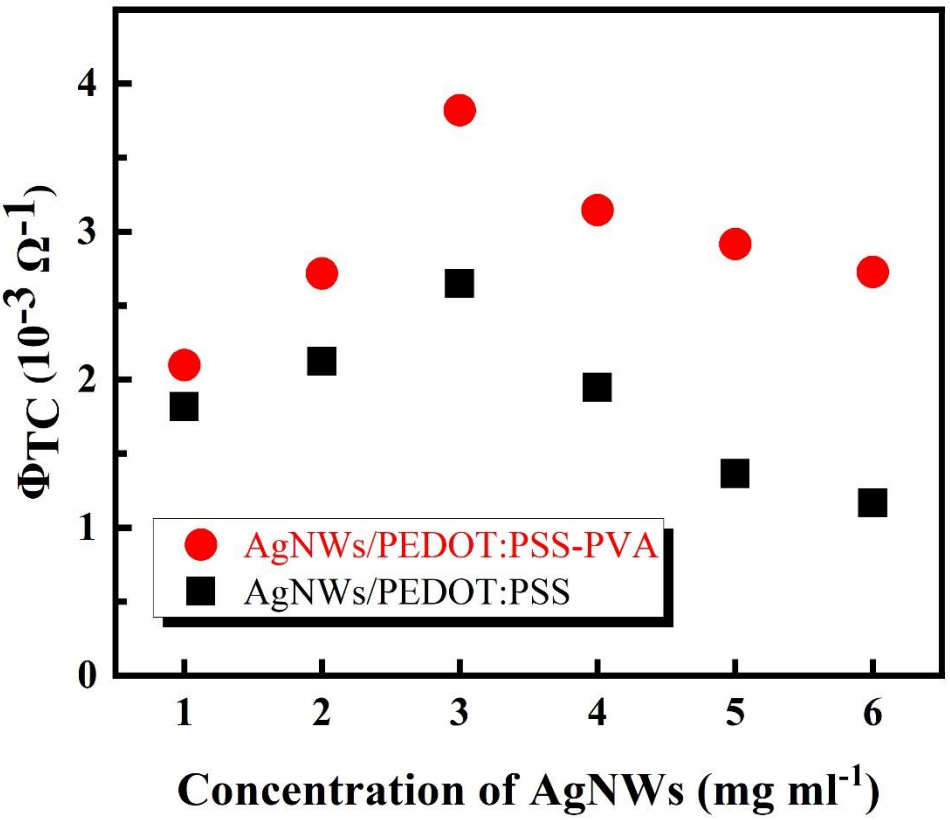

Figure 3. Φ_{TC} values of AgNWs/PEDOT:PSS and AgNWs/PEDOT:PSS-PVA electrodes as a function of AgNWs suspension concentration (1 mg/ml to 6 mg/ml).

As shown in **Figure 3** and **Table 1,** the maximum Φ_{TC} values are obtained at the concentration of 3 mg/ml AgNWs for both coatings, $\Phi_{TC} = 3.819\times10^{-3}\ \Omega^{-1}$ (Transmittance = 81.39%, $R_s = 33.4\ \Omega\ sq^{-1}$) for AgNWs/PEDOT:PSS-PVA and $\Phi_{TC} = 2.646\times10^{-3}\ \Omega^{-1}$ (Transmittance = 84.52%, $R_s = 70.3\ \Omega\ sq^{-1}$) for AgNWs/PEDOT:PSS. For all the concentrations of AgNWs, PEDOT:PSS-PVA coating layer outperforms the PEDOT:PSS.

Table 1. Optoelectronic characterization parameters of transparent electrodes

AgNWs Concentration (mg/ml)	PEDOT:PSS Coating Film			PEDOT:PSS-PVA Coating Film		
	R_S (Ωsq^{-1})	Transmittance at 550nm (%)	Φ_{TC} ($10^{-3}\ \Omega^{-1}$)	R_S (Ωsq^{-1})	Transmittance at 550nm (%)	Φ_{TC} ($10^{-3}\ \Omega^{-1}$)
1	167.5	88.79	1.818	104	85.87	2.095
2	105.43	86.1	2.123	52.7	82.33	2.715
3	70.3	84.52	2.646	33.4	81.39	3.819
4	62.4	80.99	1.945	23.8	77.16	3.143
5	56.2	77.34	1.362	19.6	75.11	2.915
6	47.3	74.83	1.163	14.3	72.29	2.725

Higher conductivity level of AgNWs/PEDOT:PSS-PVA electrode compare to AgNWs/PEDOT:PSS can be attributed to several reasons. The first is due to higher conductivity of the PEDOT:PSS-PVA film versus PEDOT:PSS film which increases the overall conductivity of the bilayer electrode (law of mixtures). The second is due to the improvement of the welding process of the nanowires at the points of attachment. One of the biggest obstacles to increasing the conductivity of AgNWs-based electrodes is the presence of an insulating polymer chain (PVP) that wraps around the silver nanowires during the chemical synthesis. The presence of this insulating layer prevents the transfer of electrons from one nanowire to another and creates high resistance at cross junction points [12,52,53]. Addition of PVA to the PEDOT:PSS increases the adhesion and cohesion forces in the coating layer. these promoted forces enhance the welding process of the nanowires at the contact points while pushing away PVP and increases the effective contact surface of AgNWs.These phenomena are originated from formation of coordination complexation of Ag←:O between PVA and AgNWs [54] and hydrogen bonding between PEDOT:PSS and PVA chains. **Figure 4(a)** and **(b)**, show the SEM images of both types of

electrodes with PEDOT:PSS and PEDOT:PSS-PVA conductive coating layers respectively. In both figures, the cross junctions of nanowires are marked with red circles. Reinforced welding and compression of AgNWs on cross junctions by PEDOT:PSS-PVA coating layer is visible in SEM images in **Figure 4(b)**.

Reinforcement of AgNWs welding in addition to increasing the conductivity, reduces surface roughness. By applying PEDOT:PSS coating on the AgNWs film, the surface roughness value range, decreases from the average root mean square (RMS) = 59.7 nm to RMS = 18.4 nm, and with the modified coating layer with PVA, the surface roughness value range decreases from RMS = 59.7 nm to RMS = 12.9 nm (detailed in **SI, Figure S3**).

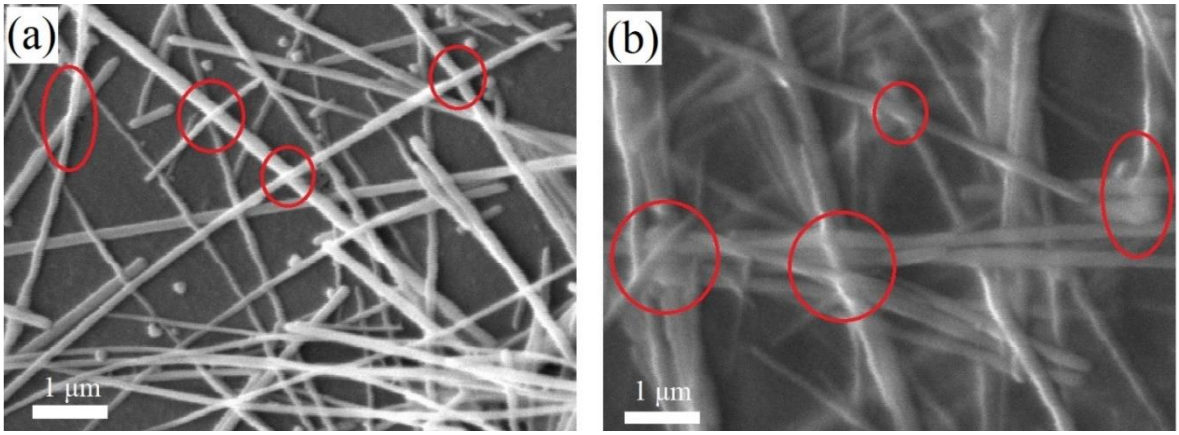

Figure 4. SEM image of **(a)** AgNWs/PEDOT:PSS electrode **(b)** AgNWs/PEDOT:PSS-PVA electrode.(The welding of the nanowires is identified in both images with red circles).

To evaluate the mechanical properties of electrodes, the relative sheet resistance (R_S/R_{S0}) changing procedures of the electrodes under static and dynamic mechanical bending test are shown in **Figure 5(a)** and **(b)** respectively.

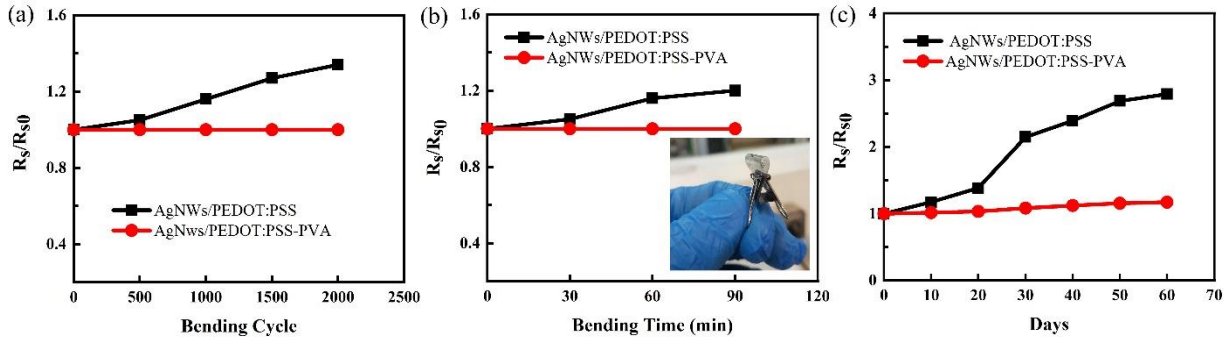

Figure 5. The normalized sheet resistance of electrodes **(a)** versus bending cycle with bending radius 0.5 mm on PET substrate **(b)** versus bending time under 180˚ bending on PET substrate (Including flexible electrode image). **(c)** versus time in the ambient condition

In both tests, mechanical properties improvement of electrodes with the modified coating is verified. This improvement is related to two different mechanisms: firstly, as mentioned earlier addition of PVA to the PEDOT:PSS, increases the adhesion and cohesion forces in the coating layer. This reinforcement not only improves welding on cross junctions of nanowires, but also maintains the arrangement and orientation of AgNWs under the mechanical stresses. Secondly, as shown in **Figure 6(a),** PEDOT:PSS film is brittle in its natural form and it breaks under severe mechanical stresses [25,27]. **Figure 6(b),** shows the SEM images from defects that have been created after 2,000 bending cycles in an electrode with PEDOT:PSS coating layer. Cracks and defects created in the PEDOT:PSS layer reduce the electrical and mechanical properties. As shown in **Figure 6(c)**, Addition of PVA as a polymer-surfactant changes PEDOT:PSS film behavior from brittle to ductile. The change of behavior is due to the dual functionality of PVA as a surfactant and as a soft polymer at the same time. PVA as a surfactant changes configuration of PEDOT:PSS from coil to fibrillar structure [11,22] and as a soft polymer swells PEDOT:PSS [55] and forms hydrogen bonds with it [56,57]. Changing the behavior of the polymer coating to the dactylic state reinforces the polymer film against severe stresses. **Figure 6(d)** shows SEM images of the electrode with PEDOT:PSS-PVA coating layer after 2,000 bending cycles. By comparing the SEM images of **Figure 6(b)** and **(d)**, reinforcement of the coating layer by addition of PVA is proved.

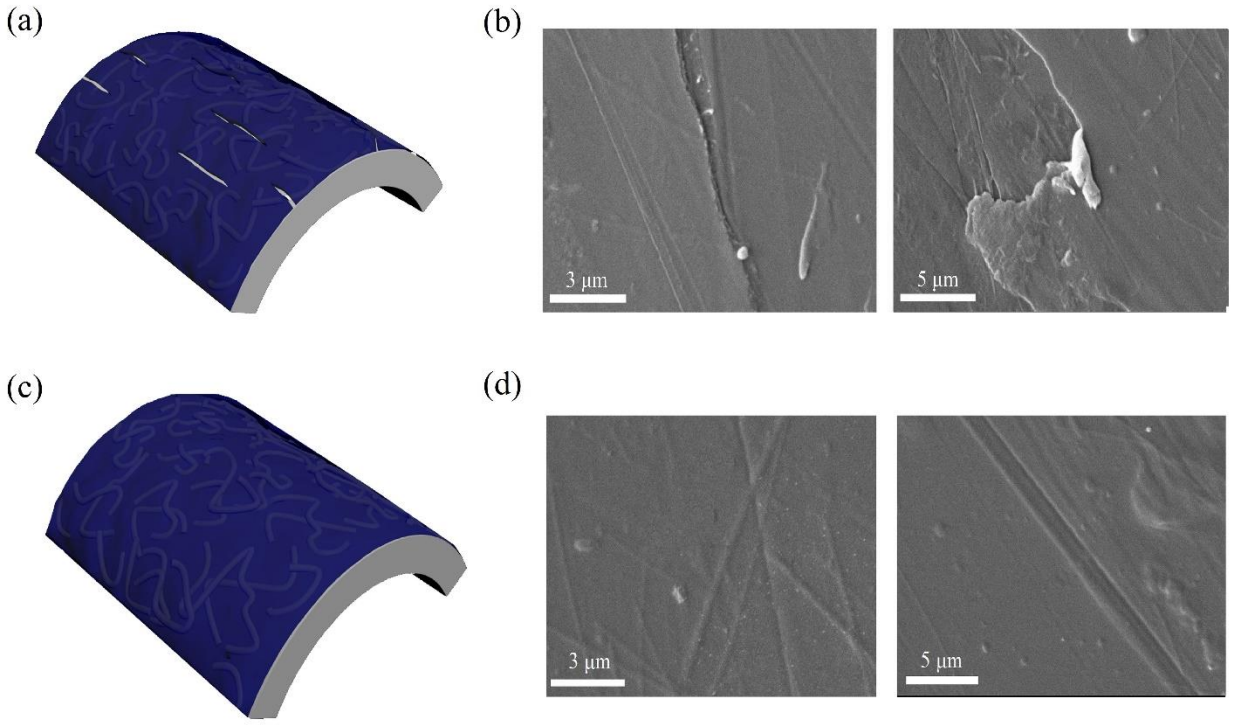

Figure 6. (a) Schematic of multiple cracks is created in bending AgNWs/PEDOT:PSS electrode **(b)** SEM images of the electrode with PEDOT:PSS coating after 2,000 bending cycles. **(c)** Schematic of the bending AgNWs/PEDOT:PSS-PVA. **(d)** SEM images of the electrode with PEDOT:PSS-PVA coating after 2,000 bending cycles.

The oxidation rate of silver nanowires increases at presence of polar water molecules and oxygen[58,59]. Another essential responsibility of coating film on top of the AgNWs in bilayer electrode is the reduction of silver nanostructures oxidation rate exposed to ambient condition [12,25,58–62]. To compare the performance of coatings as a protection layer of nanowires against oxidation, sheet resistance of the electrodes was measured every 10 days at room temperature (25°C) and an average relative humidity of 70% for 60 days. As shown in **Figure 5(c)**, sheet resistance of AgNWs/PEDOT:PSS electrode increases about 280% whereas the increase in modified coating electrode is limited to less than 20% during the 60 days. Enhancement of protective properties of PEDOT:PSS by addition of PVA in this criterion is due to the decrease of permeability of polymer film against oxygen and humidity. Reduced polymer permeability as

previously explained is associated with increased polymer packing by addition of PVA due to increased crystallinity and strong hydrogen bond formed between the polymer chains.

3.3. Investigating the performance of electrodes designed in PSCs

In order to compare the effect of polymer coatings, bilayer electrodes of AgNWs/PEDOT:PSS and AgNWs/PEDOT:PSS-PVA, as well as single-layer electrode of AgNWs, were used in the PSCs. The current density-voltage (J−V) curves and schematic structure of the prepared PCSs are shown in **Figure 7. Table 2** illustrates the current density-voltage (J−V) characteristics of the PSCs. The PSC has made with the single layer AgNWs electrode shows lower short-circuit current density (Jsc) and open-circuit voltage (V_{OC}) than the PSCs which have made with bilayer electrodes. As shown in **Table 2** in the case of AgNWs electrode, PSC shows an open-circuit voltage (Voc) of 0.55 V, short- circuit current density (Jsc) of 5.9 $mAcm^{-2}$, and fill factor (FF) of 0.46, resulting in power conversion efficiency (PCE) of 1.51%. In the case of bilayer electrodes with PEDOT:PSS and PEDOT:PSS-PVA coating layers, PSCs show same open-circuit voltages (Voc) of 0.72V, short- circuit current densities (Jsc) of 6.73 and 7.59 $mAcm^{-2}$, and fill factors (FF) of 0.61 and 0.65 and power conversion efficiencies (PCE) of 2.9% and 3.5% respectively.

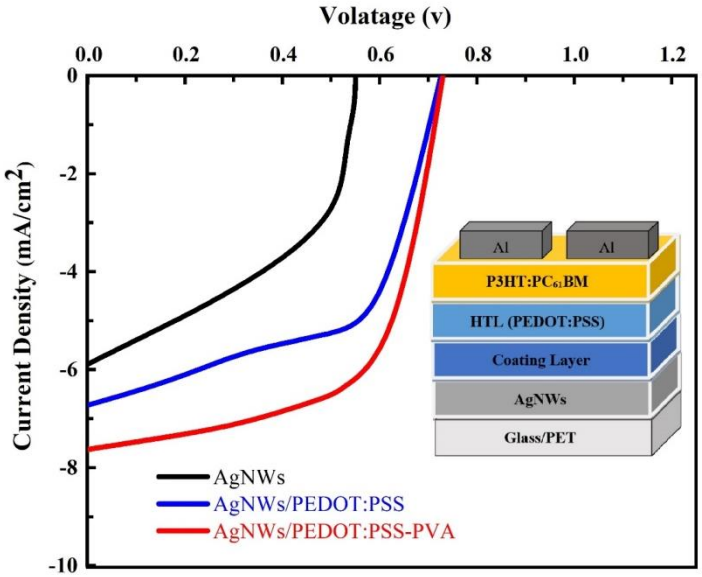

Figure 7. Current density-voltage graph of polymer solar cells based on AgNWs, AgNWs/PEDOT:PSS and AgNWs/PEDOT:PSS-PVA electrodes.

Table 2. Summarized device performances of PSCs

Electrodes used in OSCs	V_{OC} (V)	J_{SC} (mA/cm^2)	FF	PCE (%)
AgNWs	0.55	5.9	0.46	1.51
AgNWs/PEDOT:PSS	0.72	6.73	0.61	2.9
AgNWs/PEDOT:PSS-PVA	0.72	7.59	0.65	3.5

The above results show that the presence of coating layers improves the overall performance of the electrode and thus enhances the performance of the optoelectronic devices. One of the improvements in the performance of bilayer electrodes compared to the single-layer AgNWs electrode is related to the increase in Voc. Many parameters such as electrode work function, density of state (DOS) distribution or energetic disorder, charge transfer (CT) states, microstructure, D/A interface area and … affect the Voc [63]. One of the important parameters is the kind of contacts between the electrodes and the active layer which is determined by the difference between the Fermi level of the electrodes and $E_{HOMO,D}$ (energy level of highest occupied molecular orbital of donor) or $E_{LUMO,A}$ (energy level of lowest unoccupied molecular orbital of donor) of active layer. For Ohmic contact, under thermal equilibrium, the Fermi level of the electrodes will be levelled and pinned to the LUMO/HOMO level of active layer and disorder tends to be lower when contacts are Ohmic [63,64]. In the bilayer electrodes, in addition to the HTL, a coating layer (PEDOT:PSS (Clevios™ PH 1000)) with higher conductivity and lower Fermi level was used to improve the ohmic-contact between the HTL and silver nanowires. The presence of this coating layer, in addition to improving the performance of electrode and ohmic-contact, creates a good adhesion between the electrode and the HTL, which also causes less structural defects. We believe that the coating layer with the above mechanisms can lead to an increase in Voc compared to conventional polymer solar cells. Besides, annealing at low temperatures and the resulting molecular arrangement of active layer could be another reason for the high Voc of PSCs[65]. But AgNWs electrode is unable to collect holes quickly because of existing empty spaces between the nanowires and weak welding on cross junctions of AgNWs. So the remaining holes weaken the internal electric field and finally depress V_{OC} in PSCs with single-

layer electrode [22,63]. By comparing the intensity of the J_{SC}, it can be seen that due to the higher conductivity of AgNWs/PEDOT:PSS-PVA electrode, hole transfer is more efficient [66,67]. Another critical factor for better performance of the electrode with PEDOT:PSS-PVA coating layer in polymer solar cell is related to fewer defects, due to improved processability as a result of better adhesion of the coating to the sublayer [62].

4. CONCLUSION

In conclusion, a bilayer electrode with AgNWs and novel coating layer was introduced. The new coating layer is made by addition of DMSO and polymer-surfactant of PVA to the PEDOT:PSS. The presence of PVA in the coating layer significantly improves the mechanical properties of the coating and changes its nature from brittle to ductile. The use of novel coating layer increases conductivity and longevity of bilayer electrode. The addition of polymer-surfactant to the polymer coating layer improves the optoelectronic properties of bilayer electrode and increases figure of merit from $\Phi_{TC} = 2.646\times10^{-3}\ \Omega^{-1}$ to $3.819\times10^{-3}\ \Omega^{-1}$. The use of AgNWs/PEDOT:PSS-PVA electrode instead of AgNWs/PEDOT:PSS in PSC structure results 17% increase in final PCE. This improvement is attributed to better optoelectronic performance and lower structural defects in the modified electrode.

5. SUPPORTING INFORMATOIN

The Supporting Information is available free of charge on the website.

6. AUTHOR INFORMATION

Corresponding Authors:

E-mail: afshar@aut.ac.ir (Faramarz Afshar-Taromi), h.sharifi1989@gmail.com (Hamed Sharifi Dehsari)

7. REFERENCES

[1] D.S. Hecht, L. Hu, G. Irvin, Emerging Transparent Electrodes Based on Thin Films of

Carbon Nanotubes, Graphene, and Metallic Nanostructures, Adv. Mater. 23 (2011) 1482–1513. https://doi.org/10.1002/adma.201003188.

[2] M. Oh, W. Jin, H. Jeong, M. Jeong, J. Kang, H.K.-S. reports, undefined 2015, Silver nanowire transparent conductive electrodes for high-efficiency III-nitride light-emitting diodes, Nature.Com. (n.d.). https://www.nature.com/articles/srep13483 (accessed June 6, 2019).

[3] K. Ellmer, Past achievements and future challenges in the development of optically transparent electrodes, Nat. Photonics. 6 (2012) 809–817. https://doi.org/10.1038/nphoton.2012.282.

[4] D. Langley, G. Giusti, C. Mayousse, C. Celle, D. Bellet, J.-P. Simonato, Flexible transparent conductive materials based on silver nanowire networks: a review, Nanotechnology. 24 (2013) 452001. https://doi.org/10.1088/0957-4484/24/45/452001.

[5] S. Sharma, S. Shriwastava, S. Kumar, … K.B.-O.-E., undefined 2018, Alternative transparent conducting electrode materials for flexible optoelectronic devices, Elsevier. (n.d.). https://www.sciencedirect.com/science/article/pii/S1230340217301671 (accessed June 6, 2019).

[6] L. Lian, D. Dong, D. Feng, G. He, Low roughness silver nanowire flexible transparent electrode by low temperature solution-processing for organic light emitting diodes, Org. Electron. 49 (2017) 9–18. https://doi.org/10.1016/J.ORGEL.2017.06.027.

[7] N. Ferrer-Anglada, J. Pérez-Puigdemont, J. Figueras, M.Z. Iqbal, S. Roth, Flexible, transparent electrodes using carbon nanotubes, Nanoscale Res. Lett. 7 (2012) 571. https://doi.org/10.1186/1556-276X-7-571.

[8] C. Cai, F. Jia, A. Li, F. Huang, Z. Xu, L. Qiu, Y. Chen, G. Fei, M. Wang, Crackless transfer of large-area graphene films for superior-performance transparent electrodes, Carbon N. Y. 98 (2016) 457–462. https://doi.org/10.1016/J.CARBON.2015.11.041.

[9] H. Shi, C. Liu, Q. Jiang, J. Xu, Effective Approaches to Improve the Electrical Conductivity of PEDOT:PSS: A Review, Adv. Electron. Mater. 1 (2015) 1500017.

https://doi.org/10.1002/aelm.201500017.

[10] W. Cao, J. Li, H. Chen, J. Xue, Transparent electrodes for organic optoelectronic devices: a review, J. Photonics Energy. 4 (2014) 040990. https://doi.org/10.1117/1.JPE.4.040990.

[11] S. Kim, S.J. Lee, S. Cho, S. Shin, U. Jeong, J.-M. Myoung, Improved stability of transparent PEDOT:PSS/Ag nanowire hybrid electrodes by using non-ionic surfactants, Chem. Commun. 53 (2017) 8292–8295. https://doi.org/10.1039/C7CC02557B.

[12] Q. Xu, T. Song, W. Cui, Y. Liu, W. Xu, S.-T. Lee, B. Sun, Solution-Processed Highly Conductive PEDOT:PSS/AgNW/GO Transparent Film for Efficient Organic-Si Hybrid Solar Cells, ACS Appl. Mater. Interfaces. 7 (2015) 3272–3279. https://doi.org/10.1021/am508006q.

[13] X.-Y. Zeng, Q.-K. Zhang, R.-M. Yu, C.-Z. Lu, A New Transparent Conductor: Silver Nanowire Film Buried at the Surface of a Transparent Polymer, Adv. Mater. 22 (2010) 4484–4488. https://doi.org/10.1002/adma.201001811.

[14] G. Li, Z. Qiu, Y. Wang, Y. Hong, Y. Wan, J. Zhang, J. Yang, Z. Wu, W. Hong, C.F. Guo, PEDOT:PSS/Grafted-PDMS Electrodes for Fully Organic and Intrinsically Stretchable Skin-like Electronics, ACS Appl. Mater. Interfaces. 11 (2019) 10373–10379. https://doi.org/10.1021/acsami.8b20255.

[15] J. Lee, S. Connor, Y. Cui, P.P.-N. letters, undefined 2008, Solution-processed metal nanowire mesh transparent electrodes, ACS Publ. (n.d.). https://pubs.acs.org/doi/abs/10.1021/nl073296g (accessed April 7, 2019).

[16] N. Weiß, L. Müller-Meskamp, F. Selzer, L.B.-R. Advances, undefined 2015, Humidity assisted annealing technique for transparent conductive silver nanowire networks, Pubs.Rsc.Org. (n.d.). https://pubs.rsc.org/en/content/articlehtml/2015/ra/c5ra01303h (accessed April 7, 2019).

[17] L. Hu, H. Kim, J. Lee, P. Peumans, Y.C.-A. nano, undefined 2010, Scalable coating and properties of transparent, flexible, silver nanowire electrodes, ACS Publ. (n.d.). https://pubs.acs.org/doi/abs/10.1021/nn1005232 (accessed April 7, 2019).

[18] E. Garnett, W. Cai, J. Cha, F. Mahmood, S.C.-N. materials, undefined 2012, Self-limited plasmonic welding of silver nanowire junctions, Nature.Com. (n.d.). https://www.nature.com/articles/nmat3238 (accessed April 7, 2019).

[19] Y. Altin, M. Tas, İ. Borazan, A. Demir, A. Bedeloglu, Solution-processed transparent conducting electrodes with graphene, silver nanowires and PEDOT:PSS as alternative to ITO, Surf. Coatings Technol. 302 (2016) 75–81. https://doi.org/10.1016/J.SURFCOAT.2016.05.058.

[20] D. Lee, H. Lee, Y. Ahn, Y.L.- Carbon, undefined 2015, High-performance flexible transparent conductive film based on graphene/AgNW/graphene sandwich structure, Elsevier. (n.d.). https://www.sciencedirect.com/science/article/pii/S0008622314009415 (accessed January 9, 2020).

[21] R. Shimotsu, T. Takumi, V. Vohra, All solution-processed micro-structured flexible electrodes for low-cost light-emitting pressure sensors fabrication, Sci. Rep. 7 (2017). https://doi.org/10.1038/s41598-017-07284-8.

[22] E.D. Jung, Y.S. Nam, H. Seo, B.R. Lee, J.C. Yu, S.Y. Lee, J.-Y. Kim, J.-U. Park, M.H. Song, Highly efficient flexible optoelectronic devices using metal nanowire-conducting polymer composite transparent electrode, Electron. Mater. Lett. 11 (2015) 906–914. https://doi.org/10.1007/s13391-015-5120-z.

[23] T. Cheng, Y.Z. Zhang, J.P. Yi, L. Yang, J.D. Zhang, W.Y. Lai, W. Huang, Inkjet-printed flexible, transparent and aesthetic energy storage devices based on PEDOT:PSS/Ag grid electrodes, J. Mater. Chem. A. 4 (2016) 13754–13763. https://doi.org/10.1039/c6ta05319j.

[24] D.-Y. Lee, S.-I. Na, S.-S. Kim, Graphene oxide/PEDOT:PSS composite hole transport layer for efficient and stable planar heterojunction perovskite solar cells, Nanoscale. 8 (2016) 1513–1522. https://doi.org/10.1039/C5NR05271H.

[25] M. Cao, M. Wang, L. Li, H. Qiu, Z. Yang, Effect of Graphene-EC on Ag NW-Based Transparent Film Heaters: Optimizing the Stability and Heat Dispersion of Films, ACS Appl. Mater. Interfaces. 10 (2018) 1077–1083. https://doi.org/10.1021/acsami.7b14820.

[26] L. V. Kayser, D.J. Lipomi, Stretchable Conductive Polymers and Composites Based on PEDOT and PEDOT:PSS, Adv. Mater. 31 (2019) 1806133. https://doi.org/10.1002/adma.201806133.

[27] E. Dauzon, A. Mansour, … M.N.-… applied materials &, undefined 2019, Conducting and Stretchable PEDOT: PSS Electrodes: Role of Additives on Self-Assembly, Morphology and Transport, ACS Publ. (n.d.). https://pubs.acs.org/doi/abs/10.1021/acsami.9b00934 (accessed June 7, 2019).

[28] P.J. Taroni, G. Santagiuliana, K. Wan, P. Calado, M. Qiu, H. Zhang, N.M. Pugno, M. Palma, N. Stingelin-Stutzman, M. Heeney, O. Fenwick, M. Baxendale, E. Bilotti, Toward Stretchable Self-Powered Sensors Based on the Thermoelectric Response of PEDOT:PSS/Polyurethane Blends, Adv. Funct. Mater. 28 (2018) 1704285. https://doi.org/10.1002/adfm.201704285.

[29] J. Luo, D. Billep, T. Waechtler, T. Otto, … M.T.-… of M.C., undefined 2013, Enhancement of the thermoelectric properties of PEDOT: PSS thin films by post-treatment, Pubs.Rsc.Org. (n.d.). https://pubs.rsc.org/en/content/articlehtml/2013/ta/c3ta11209h (accessed April 22, 2019).

[30] N.K. Unsworth, I. Hancox, C. Argent Dearden, P. Sullivan, M. Walker, R.S. Lilley, J. Sharp, T.S. Jones, Comparison of dimethyl sulfoxide treated highly conductive poly(3,4-ethylenedioxythiophene):poly(styrenesulfonate) electrodes for use in indium tin oxide-free organic electronic photovoltaic devices, Org. Electron. 15 (2014) 2624–2631. https://doi.org/10.1016/J.ORGEL.2014.07.015.

[31] B. Fan, X. Mei, J. Ouyang, Significant Conductivity Enhancement of Conductive Poly(3,4-ethylenedioxythiophene):Poly(styrenesulfonate) Films by Adding Anionic Surfactants into Polymer Solution, Macromolecules. 41 (2008) 5971–5973. https://doi.org/10.1021/ma8012459.

[32] A. Hasani, H. Sharifi Dehsari, M. Asghari Lafmejani, A. Salehi, F. Afshar Taromi, K. Asadi, S.Y. Kim, Ammonia-Sensing Using a Composite of Graphene Oxide and Conducting Polymer, Phys. Status Solidi - Rapid Res. Lett. 12 (2018) 1800037.

https://doi.org/10.1002/pssr.201800037.

[33] A.S. Alshammari, Improved electrical stability of silver NWs based hybrid transparent electrode interconnected with polymer functionalized CNTs, Mater. Res. Bull. 111 (2019) 245–250. https://doi.org/10.1016/j.materresbull.2018.11.017.

[34] X. Fan, W. Nie, H. Tsai, N. Wang, H. Huang, Y. Cheng, R. Wen, L. Ma, F. Yan, Y. Xia, PEDOT:PSS for Flexible and Stretchable Electronics: Modifications, Strategies, and Applications, Adv. Sci. 6 (2019). https://doi.org/10.1002/advs.201900813.

[35] S. Savagatrup, E. Chan, S.M. Renteria-Garcia, A.D. Printz, A. V. Zaretski, T.F. O'Connor, D. Rodriquez, E. Valle, D.J. Lipomi, Plasticization of PEDOT:PSS by common additives for mechanically robust organic solar cells and wearable sensors, Adv. Funct. Mater. 25 (2015) 427–436. https://doi.org/10.1002/adfm.201401758.

[36] Y. Sun, B. Mayers, T. Herricks, Y. Xia, Polyol Synthesis of Uniform Silver Nanowires: A Plausible Growth Mechanism and the Supporting Evidence, Nano Lett. 3 (2003) 955–960. https://doi.org/10.1021/nl034312m.

[37] P. Lee, J. Lee, H. Lee, J. Yeo, S. Hong, K.H. Nam, D. Lee, S.S. Lee, S.H. Ko, Highly Stretchable and Highly Conductive Metal Electrode by Very Long Metal Nanowire Percolation Network, Adv. Mater. 24 (2012) 3326–3332. https://doi.org/10.1002/adma.201200359.

[38] L. Wang, T. Zhang, … S.Z.-N., undefined 2012, Two-dimensional ultrathin gold film composed of steadily linked dense nanoparticle with surface plasmon resonance, Nanoscalereslett.Springeropen.Com. (n.d.). https://nanoscalereslett.springeropen.com/articles/10.1186/1556-276X-7-683 (accessed April 23, 2021).

[39] S. Sahare, N. Veldurthi, S. Datar, T. Bhave, Photon assisted conducting atomic force microscopy study of nanostructured additives in P3HT:PCBM, RSC Adv. 5 (2015) 102795–102802. https://doi.org/10.1039/c5ra20266c.

[40] G. Haacke, New figure of merit for transparent conductors, J. Appl. Phys. 47 (1976) 4086–

4089. https://doi.org/10.1063/1.323240.

[41] A. Hasani, H. Sharifi Dehsari, M. Asghari Lafmejani, A. Salehi, F. Afshar Taromi, K. Asadi, S.Y. Kim, Ammonia-Sensing Using a Composite of Graphene Oxide and Conducting Polymer, Phys. Status Solidi - Rapid Res. Lett. 12 (2018) 1800037. https://doi.org/10.1002/pssr.201800037.

[42] X. Fan, J. Wang, H. Wang, X. Liu, H. Wang, Bendable ITO-free Organic Solar Cells with Highly Conductive and Flexible PEDOT:PSS Electrodes on Plastic Substrates, ACS Appl. Mater. Interfaces. 7 (2015) 16287–16295. https://doi.org/10.1021/acsami.5b02830.

[43] T.A. Yemata, A.K.K. Kyaw, Y. Zheng, X. Wang, Q. Zhu, W.S. Chin, J. Xu, Enhanced thermoelectric performance of poly(3,4- ethylenedioxythiophene):poly(4-styrenesulfonate) (PEDOT:PSS) with long- term humidity stability via sequential treatment with trifluoroacetic acid, Polym. Int. 69 (2020) 84–92. https://doi.org/10.1002/pi.5921.

[44] J. Ouyang, Q. Xu, C. Chu, Y. Yang, G. Li, J.S.- Polymer, undefined 2004, On the mechanism of conductivity enhancement in poly (3, 4-ethylenedioxythiophene): poly (styrene sulfonate) film through solvent treatment, Elsevier. (n.d.). https://www.sciencedirect.com/science/article/pii/S0032386104009668 (accessed November 18, 2020).

[45] N. Kim, B.H. Lee, Role of Interchain Coupling in the Metallic State of Conducting Polymers Organic solar cells View project Metal Oxides View project, Artic. Phys. Rev. Lett. 109 (2012). https://doi.org/10.1103/PhysRevLett.109.106405.

[46] N. Kim, S. Kee, S.H. Lee, B.H. Lee, Y.H. Kahng, Y.R. Jo, B.J. Kim, K. Lee, Highly conductive PEDOT:PSS nanofibrils induced by solution-processed crystallization, Adv. Mater. 26 (2014) 2268–2272. https://doi.org/10.1002/adma.201304611.

[47] E. Hosseini, V. Kollath, K.K.-J. of M.C. C, undefined 2020, The key mechanism of conductivity in PEDOT: PSS thin films exposed by anomalous conduction behaviour upon solvent-doping and sulfuric acid post-treatment, Pubs.Rsc.Org. (n.d.). https://pubs.rsc.org/en/content/articlehtml/2020/tc/c9tc06311k (accessed December 5, 2020).

[48] A. Lenz, H. Kariis, A. Pohl, P. Persson, L.O.-C. physics, undefined 2011, The electronic structure and reflectivity of PEDOT: PSS from density functional theory, Elsevier. (n.d.). https://www.sciencedirect.com/science/article/pii/S0301010411001571 (accessed December 6, 2020).

[49] D. Mengistie, P. Wang, C.C.-J. of M.C. A, undefined 2013, Effect of molecular weight of additives on the conductivity of PEDOT: PSS and efficiency for ITO-free organic solar cells, Pubs.Rsc.Org. (n.d.). https://pubs.rsc.org/en/content/articlehtml/2013/ta/c3ta11726j (accessed May 15, 2019).

[50] H.S. Biswal, P.R. Shirhatti, S. Wategaonkar, O−H···O versus O−H···S Hydrogen Bonding I: Experimental and Computational Studies on the *p* -Cresol·H $_2$ O and *p* -Cresol·H $_2$ S Complexes, J. Phys. Chem. A. 113 (2009) 5633–5643. https://doi.org/10.1021/jp9009355.

[51] Y.T. Tseng, Y.C. Lin, C.C. Shih, H.C. Hsieh, W.Y. Lee, Y.C. Chiu, W.C. Chen, Morphology and properties of PEDOT:PSS/soft polymer blends through hydrogen bonding interaction and their pressure sensor application, J. Mater. Chem. C. 8 (2020) 6013–6024. https://doi.org/10.1039/d0tc00559b.

[52] J. Hwang, Y. Shim, S. Yoon, S. Lee, S.P.-R. advances, undefined 2016, Influence of polyvinylpyrrolidone (PVP) capping layer on silver nanowire networks: theoretical and experimental studies, Pubs.Rsc.Org. (n.d.). https://pubs.rsc.org/en/content/articlehtml/2016/ra/c5ra28003f (accessed April 23, 2021).

[53] F.; Selzer, C.; Floresca, D.; Kneppe, L.; Bormann, C.; Sachse, N.; Weiß, A.; Eychmüller, A.; Amassian, L.; Müller-Meskamp, K. Leo, Electrical limit of silver nanowire electrodes: Direct measurement of the nanowire junction resistance Item Type Article, Aip.Scitation.Org. 108 (2016). https://doi.org/10.1063/1.4947285.

[54] X. Wang, J. Zhou, Y. Zhu, W. Cheng, D. Zhao, … G.X.-C.E., undefined 2019, Assembly of silver nanowires and PEDOT: PSS with hydrocellulose toward highly flexible, transparent and conductivity-stable conductors, Elsevier. (n.d.). https://www.sciencedirect.com/science/article/pii/S1385894719330591 (accessed January 15, 2020).

[55] P. Li, K. Sun, J. Ouyang, Stretchable and Conductive Polymer Films Prepared by Solution Blending, ACS Appl. Mater. Interfaces. 7 (2015) 18415–18423. https://doi.org/10.1021/acsami.5b04492.

[56] Y. Zhang, M. Guo, Y. Zhang, C. Tang, C.J.-P. Testing, undefined 2020, Flexible, stretchable and conductive PVA/PEDOT: PSS composite hydrogels prepared by SIPN strategy, Elsevier. (n.d.). https://www.sciencedirect.com/science/article/pii/S014294181931462X (accessed January 16, 2020).

[57] C. Chen, A. Torrents, L. Kulinsky, R. Nelson, M.M.-S. Metals, undefined 2011, Mechanical characterizations of cast Poly (3, 4-ethylenedioxythiophene): Poly (styrenesulfonate)/Polyvinyl Alcohol thin films, Elsevier. (n.d.). https://www.sciencedirect.com/science/article/pii/S0379677911003729 (accessed May 27, 2019).

[58] J.L. Elechiguerra, L. Larios-Lopez, C. Liu, D. Garcia-Gutierrez, A. Camacho-Bragado, M.J. Yacaman, Corrosion at the nanoscale: The case of silver nanowires and nanoparticles, Chem. Mater. 17 (2005) 6042–6052. https://doi.org/10.1021/cm051532n.

[59] Y.-Y. Yu, Y.-J. Ting, C.-L. Chung, T.-W. Tsai, C.-P. Chen, Comprehensive Study on Chemical and Hot Press-Treated Silver Nanowires for Efficient Polymer Solar Cell Application, Mdpi.Com. (2017). https://doi.org/10.3390/polym9110635.

[60] G. Cai, P. Darmawan, M. Cui, J. Wang, J. Chen, S. Magdassi, P.S. Lee, Highly Stable Transparent Conductive Silver Grid/PEDOT:PSS Electrodes for Integrated Bifunctional Flexible Electrochromic Supercapacitors, Adv. Energy Mater. 6 (2016) 1501882. https://doi.org/10.1002/aenm.201501882.

[61] J. Miao, S. Chen, H. Liu, X.Z.-C.E. Journal, undefined 2018, Low-temperature nanowelding ultrathin silver nanowire sandwiched between polydopamine-functionalized graphene and conjugated polymer for highly stable and, Elsevier. (n.d.). https://www.sciencedirect.com/science/article/pii/S1385894718305023 (accessed May 27, 2019).

[62] A.G. Ricciardulli, S. Yang, G.-J.A.H. Wetzelaer, X. Feng, P.W.M. Blom, Hybrid Silver Nanowire and Graphene-Based Solution-Processed Transparent Electrode for Organic Optoelectronics, Adv. Funct. Mater. 28 (2018) 1706010. https://doi.org/10.1002/adfm.201706010.

[63] N. Elumalai, A.U.-E.& E. Science, undefined 2016, Open circuit voltage of organic solar cells: an in-depth review, Pubs.Rsc.Org. (n.d.). https://pubs.rsc.org/en/content/articlehtml/2015/ee/c5ee02871j (accessed June 6, 2019).

[64] P.W.M.; Blom, V.D.; Mihailetchi, L.; Koster, D.E. Markov, P.W.M. Blom, V.D. Mihailetchi, L.J.A. Markov, P.W.M. Blom, V.D. Mihailetchi, L. Jan, A. Koster, Device physics of polymer Device Physics of Polymer:Fullerene Bulk Heterojunction Solar Cells**, Wiley Online Libr. 19 (2018) 1551–1566. https://doi.org/10.1002/adma.200601093.

[65] P. Vanlaeke, A. Swinnen, I. Haeldermans, G. Vanhoyland, T. Aernouts, D. Cheyns, C. Deibel, J. D'Haen, P. Heremans, J. Poortmans, J. V. Manca, P3HT/PCBM bulk heterojunction solar cells: Relation between morphology and electro-optical characteristics, Sol. Energy Mater. Sol. Cells. 90 (2006) 2150–2158. https://doi.org/10.1016/j.solmat.2006.02.010.

[66] B. Rezaei, F. Afshar-Taromi, Z. Ahmadi, S.A.-R.-O. Materials, undefined 2019, High conductive ITO-free flexible electrode based on Gr-grafted-CNT/Au NPs for optoelectronic applications, Elsevier. (n.d.). https://www.sciencedirect.com/science/article/pii/S092534671930076X (accessed June 6, 2019).

[67] D. Lee, H. Lee, Y. Ahn, Y. Jeong, D. Lee, Y.L.- Nanoscale, undefined 2013, Highly stable and flexible silver nanowire–graphene hybrid transparent conducting electrodes for emerging optoelectronic devices, Pubs.Rsc.Org. (n.d.). https://pubs.rsc.org/en/content/articlehtml/2013/nr/c3nr02320f (accessed June 6, 2019).